ADVANCED FUNCTIONAL MATERIALS
www.afm-journal.de

H-Aggregation Strategy in the Design of Molecular Semiconductors for Highly Reliable Organic Thin Film Transistors

Seul-ong Kim, Tae Kyu An, Jun Chen, Il Kang, So Hee Kang, Dae Sung Chung, Chan Eon Park, Yun-Hi Kim,* and Soon-Ki Kwon**

Four new quaterthiophene derivatives with end-groups composed of dicyclohexyl ethyl (DCE4T), dicyclohexyl butyl (DCB4T), cyclohexyl ethyl (CE4T), and cyclohexyl butyl (CB4T) were designed. All materials showed high solubility in common organic solvents. UV–vis absorption measurements showed that the quaterthiophene derivatives with asymmetrically substituted cyclohexyl end-groups (CE4T and CB4T) preferred H-type aggregation whereas those with symmetrically substituted cyclohexyl end-groups (DCE4T and DCB4T) preferred J-type aggregation. The molecular structure-dependent packing (H or J) of the new quaterthiophene derivatives was analyzed by grazing-incidence wide-angle X-ray scattering (GIWAXS) measurements. The field-effect mobilities of devices that incorporated the asymmetrical molecules, CE4T and CB4T, were quite high, above 10^{-2} cm^2 V^{-1} s^{-1}, due to H-aggregation, whereas the field-effect mobilities of devices that incorporated symmetrical molecules, DCE4T and DCB4T, were poor, below 10^{-4} cm^2 V^{-1} s^{-1}, due to J-aggregation. More importantly, H-aggregation within the thin film provided stable crystalline morphologies in the spin-coated films, and, thus, thin film transistors (TFTs) using cyclohexylated quaterthiophenes yielded highly reproducible transistor performances. The distributions of measured field-effect mobilities in transistors based on cyclohexylated quaterthiophenes with H-aggregation were remarkably narrow.

1. Introduction

Over the past decade, several conjugated organic oligomers and polymers have been developed for potential use in low-cost semiconductor applications to replace their higher-cost inorganic counterparts. The most attractive aspect of these organic materials is that their structures can be diversified and their physical or chemical properties tuned through strategic molecular design.[1–9]

Among the variety of organic semiconductors developed, thiophene-based materials have emerged as an important class because of their high chemical and electrochemical stability, the accessibility of their preparation for thiophene synthesis, and the availability of well-developed/regioselective ring–ring coupling methodologies.[10,11] Furthermore, the properties of oligo/polythiophene cores can be efficiently tuned by introducing appropriate substitutions. To date, the field-effect transistor (FET) mobilities in devices composed of oligomeric thiophene semiconductors are generally higher than those obtained from conjugated polymers. Oligomeric thiophene semiconductor polymers engage in long-range packing, and efficient charge transport is directly related to the long-range packing of molecules in semiconductor films. Many synthetic methods have been developed to functionalize the α- and ω-ends of conjugated thiophene ring systems to increase the solubility and stability toward oxidation or to influence the solid-state ordering of oligothiophenes without affecting the planarity of the conjugated backbone.[12,13]

The present study was devised based on the following three considerations: i) previously reported organic semiconductors have generally shown J-aggregation[14] with head-to-tail molecular stacking;[15] ii) large area π-stacking between adjacent molecules can be realized by H-aggregation, which occurs when molecules stack side by side;[16] and iii) H-aggregation induces stable morphologies in thin films and reproducible transistor performances. We describe a novel synthetic strategy to induce H-aggregation between adjacent molecules in the thin film state. We designed four types of quaterthiophene derivative with end-groups composed of cyclohexyl ethyl (CE4T), cyclohexyl butyl (CB4T), dicyclohexyl ethyl (DCE4T), and dicyclohexyl butyl (DCB4T). UV–vis absorption and grazing-incidence wide-angle X-ray scattering (GIWAXS) analyses indicated that the asymmetric derivatives, CE4T and CB4T, tended to undergo

S.-o. Kim, J. Chen, I. Kang, Prof. S.-K. Kwon
School of Materials Science and Engineering
Engineering Research Institute
Gyeongsang National University
Jinju 660–701, Korea
E-mail: skwon@gnu.ac.kr
S. H. Kang, Prof. Y.-H. Kim
Department of Chemistry
Gyeongsang National University JinJu
600–701, Korea
E-mail: ykim@gnu.ac.kr
T. K. An, Dr. D. S. Chung, Prof. C. E. Park
Polymer Research Institute
Department of Chemical Engineering
Pohang University of Science Technology
Pohang 790–784, South Korea
E-mail: cep@postech.ac.kr

DOI: 10.1002/adfm.201002367

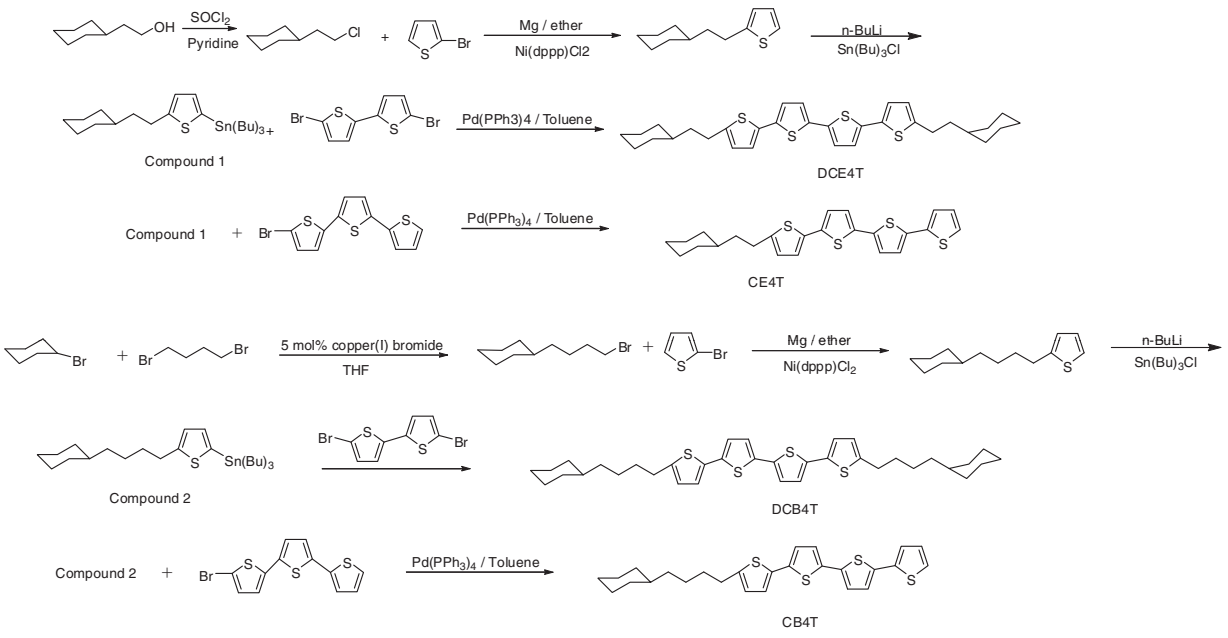

Scheme 1. Synthetic scheme for the alkyl cyclohexyl-substituted quaterthiophenes.

H-aggregation whereas the symmetric derivatives, DCE4T and DCB4T, tended to undergo J-aggregation.[14]

We fabricated a thin-film transistor using the synthesized materials as active layers. The charge carrier mobility in asymmetric molecules with H-aggregation was much higher than in symmetric molecules with J-aggregation. The correlation between structure and mobility is discussed to describe the aggregation type-dependent charge carrier mobility in detail. In addition, thin films formed by asymmetric molecules yielded a morphology that was more uniform than that of thin films formed by symmetric molecules. Therefore, transistors based on asymmetric molecules showed excellent reproducibility.

2. Results and Discussion

2.1. Synthesis

We carried out the synthesis of the cyclohexylated alkyl substituted quaterthiophenes by Grignard reaction and Stille coupling. The synthetic scheme is outlined in **Scheme 1**. The obtained quaterthiophenes were purified by recrystallization using MeOH–CH_2Cl_2 or MeOH–$CHCl_3$ and subjected to Soxhlet extraction using toluene. The quaterthiophenes were characterized by ^{1}H NMR, mass spectrometry, and elemental analysis. All quaterthiophenes were readily soluble in chloroform and other nonpolar solvents, such as toluene and benzene, whereas the previously reported dicyclohexylated quaterthiophene showed limited solubility.[1]

2.2. Thermal Analysis

The thermal properties of the synthesized quaterthiophenes were evaluated by TGA and DSC by applying a repeated heating–cooling–heating cycle under a nitrogen atmosphere. Good thermal stability is important because it conveys device longevity.[17] TGA revealed good thermal stability of the cyclohexylated alkyl substituted quaterthiophene. A 5% weight loss was observed at 305 °C for CE4T, 372 °C for DCE4T, 325 °C for CB4T, and 389.7 °C for DCB4T (Figure S1). The symmetrically substituted DCE4T and DCB4T (Figure S1) materials showed enhanced thermal stability. Interestingly, two exothermic peaks appeared in the DSC curve in a narrow temperature range for the case of the asymmetrically substituted molecules, CE4T and CB4T, compared with single peaks for the case of the symmetrically substituted molecules, DCE4T and DCB4T (Figure S2 and **Table 1**).

2.3. UV–Vis Absorption Spectroscopy

Intermolecular interactions between adjacent molecules in the solid state were characterized by UV–vis spectroscopy. We discovered that the absorption peaks of the asymmetric molecules (cyclohexylated quaterthiophenes) in thin films were blue-shifted relative to those in solution (**Figure 1**a,c and **Table 2**). This result could be explained by H-aggregation of the molecules, which was correlated with the specific molecular packing structure.[18] In other words, the cyclohexylated molecules, CE4T and

Table 1. DSC and TGA data for CE4T, DCE4T, CB4T, and DCB4T.

	CE4T	DCE4T	CB4T	DCB4T
Td (5% weight loss)	305 °C	372 °C	325 °C	389.7 °C
1st heating	146 °C	212 °C	147,157 °C	174 °C
Cooling	138,149 °C	204 °C	155 °C	164,173 °C
2nd heating	146 °C	212 °C	147,157 °C	175 °C

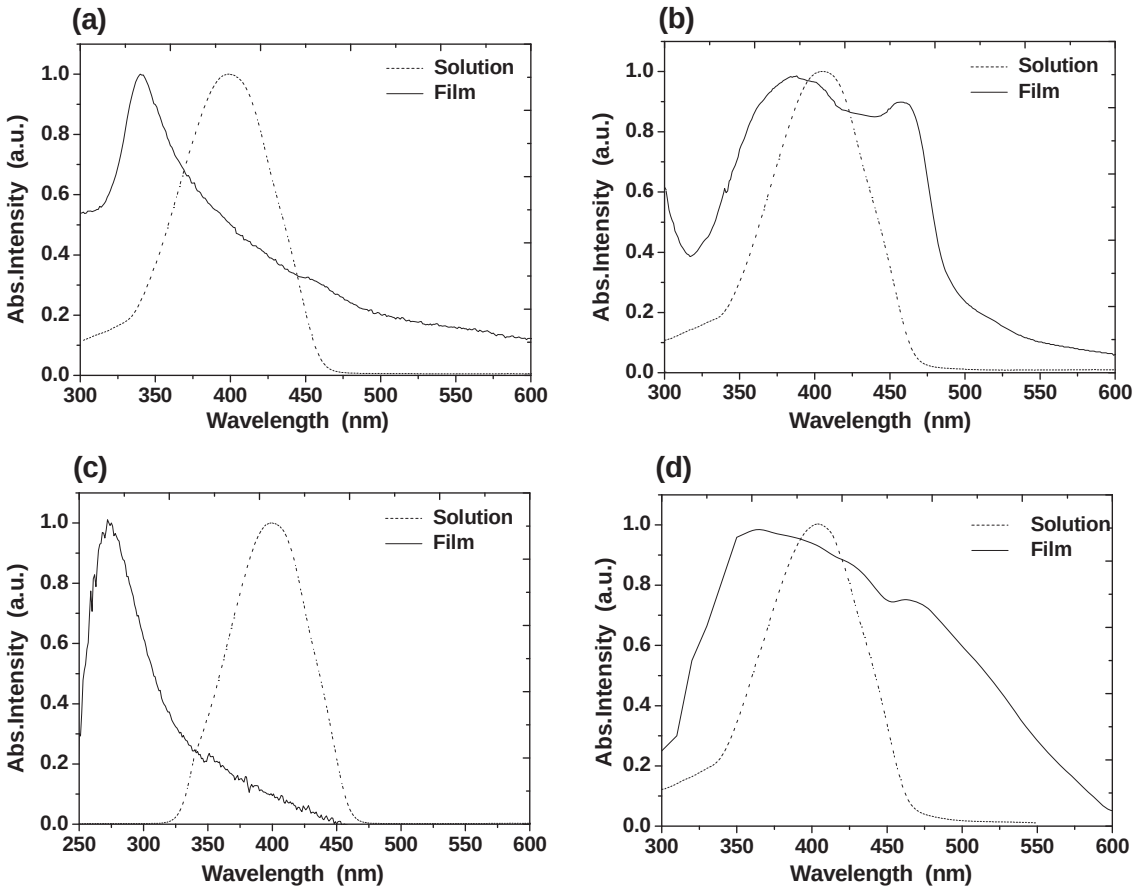

Figure 1. UV–vis absorption spectra of a) CE4T, b) DCE4T, c) CB4T, and d) DCB4T in toluene solution.

CB4T, tended to stack in parallel.[19] In contrast, the absorption peaks of the symmetric molecules (dicyclohexylated quaterthiophenes) in thin films were red-shifted relative to those in solution (Figure 1b,d and Table 2). These observations have been noted in many conventional molecular semiconductors and are explained well by J-aggregation.[14] J-aggregation is observed when molecules stack by a head-to-tail arrangement.[15]

A molecule can be approximated as a point dipole, and the potential energy of interaction between two molecules is a function of their relative dipole configuration or orientation. To calculate the potential energy of interaction between two dipoles, one dipole moment is defined by μ_1 and the other dipole is defined by μ_2, separated by a vector **r**. The potential energy of μ_2 is calculated using classical electromagnetic theory in presence of the electric field generated by the dipole moment μ_1. In the thin film systems, two assumptions are appropriate. Firstly, we can apply a Taylor expansion to the Coulomb potential because the intermolecular distance (between adjacent molecular dipoles) is very short. Secondly, the sum of charges is 0, that is, the charge distribution is neutral. Finally, the potential energy of interaction between two dipoles can be described as follows:

$$V = \frac{\mu_1 \cdot \mu_2}{4\pi\varepsilon_0 r^3} - 3\frac{(\mu_1 \cdot \mathbf{r})(\mu_2 \cdot \mathbf{r})}{4\pi\varepsilon_0 r^5} = \frac{\mu_1\mu_2(1-\cos^2\theta)}{4\pi\varepsilon_0 r^3}, \quad (1)$$

because $\mu_1 \cdot \mathbf{r} = \mu_1 r\cos\theta \mu_2 \cdot \mathbf{r} = \mu_2 r\cos\theta$, as shown in **Figure 2**a.[20]

Next, we can estimate the molecular configuration using the equation for the potential energy of interaction between two dipoles. From Equation 1, we can see that the energy of the system increases when the value of θ is close to 90° (H-aggregation) and decreases when it is close to 0° (J-aggregation). In other words, the excitonic state of the molecular aggregate splits into two energy levels, one that is higher and another that is lower than the energy of the monomer, as shown in Figure 2b, depending on the interaction between the transition dipoles.[21] Because the blue shift in the UV absorption could be interpreted as an increase in energy and the red shift in the absorption as a decrease in the energy of the excitonic energy states, the cyclohexylated quaterthiophenes were thought to

Table 2. Optical properties of CE4T, DCE4T, CB4T, and DCB4T.

		CE4T	DCE4T	CB4T	DCB4T
UV–vis [nm]	Solution	398	404	401	404
	Film	339	385, 458	269	365, 462

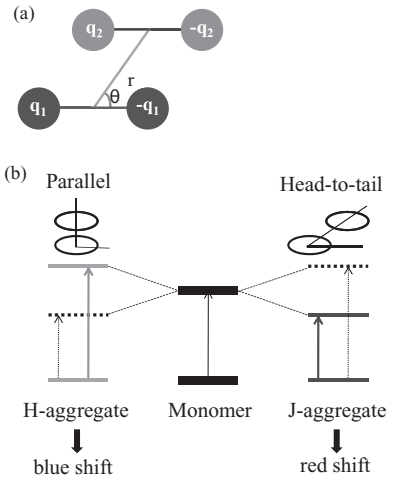

Figure 2. a) Arrangement of the molecular dipoles separated by a distance *r*. b) Scheme describing the excitonic energy state splitting, into two levels, in H-aggregated and J-aggregated materials.

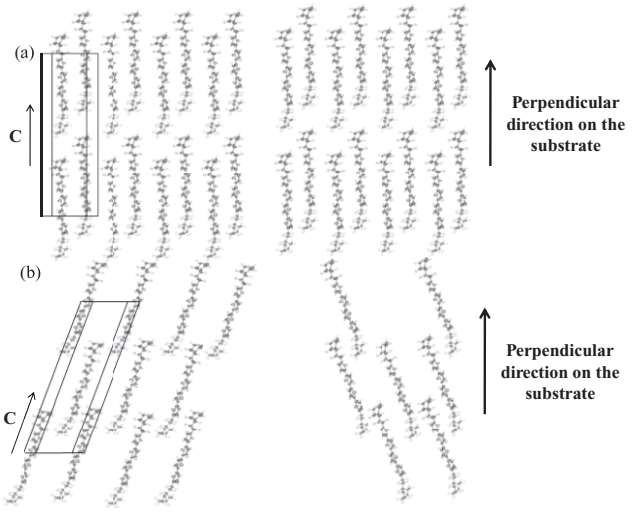

Figure 4. Estimated packing structures for a) asymmetric molecules, and b) symmetric molecules.

form H-aggregation-type molecular packing structures and dicyclohexylated quaterthiophenes were thought to form J-aggregation-type molecular packing structures, respectively.[18,19]

Previously described high-performance organic semiconductors like TIPS-pentacene and its derivatives were usually characterized by a packing type that resembled J-aggregation and not H-aggregation. However, the area of pi-overlap between adjacent molecules, which is believed to be central to enhancing the charge carrier mobility of molecular semiconductors,[16] is higher in H-aggregated materials such that they yield better charge carrier mobilities than J-aggregated materials. Although H-aggregation is difficult to achieve, as mentioned above, it can be induced through strategic molecular design. Dividing molecular semiconductors into a central group (in our cases, quaterthiophene) and side groups (cyclohexylated alkyl chain) suggests that large asymmetrically substituted side groups would favor packing of adjacent molecules in parallel so that the bulky side groups avoid proximity and minimize steric hindrance. On the other hand, dicyclohexylated quaterthiophenes stack such that molecules are tilted on the substrate (J-aggregation) to avoid bulky side groups.

The molecular packing of the designed semiconductors was examined by GIWAXS, as shown in **Figure 3**, to test the hypothesis described above. These results indicated that cyclohexylated quaterthiophenes were vertically oriented on the substrate and grew along the out-of-plane direction, as shown in **Figure 4**a.[22] Diffraction patterns of dicyclohexylated quaterthiophenes could not be observed along the out-of-plane and in-plane directions. However, diagonal diffraction patterns were observed. These diffraction results suggest that cyclohexylated quaterthiophenes are vertically aligned in a face-to-face packing structure, and dicyclohexylated quaterthiophenes are diagonally packed on the substrate, as shown in Figure 4b.[23,24]

It should be noted that cyclohexylated quaterthiophenes can engage in two types of crystal packing for a given molecular dipole, as shown in Figure 4a (compare the left and right models). The out-of-plane scattering profiles of cyclohexylated quaterthiophenes, which were extracted along the α_f-direction at $2\theta_f = 0°$ from the scattering patterns in Figure 3, showed two types of n-numbered diffraction peaks, as shown in Figure S3. The presence of two exothermic peaks for the cyclohexylated quaterthiophenes in DSC measurements (Figures S2a and c) also supports this model, because domains with different packing structures had different durabilities under thermal exposure.

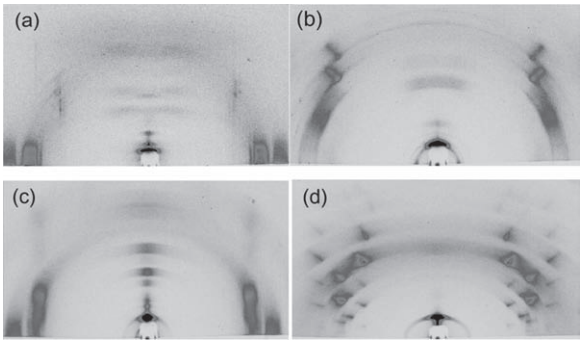

Figure 3. GIWAXS scattering results for a) CE4T, b) DCE4T, c) CB4T, and d) DCB4T.

2.4. FET Behavior

To test the potential of the quaterthiophene derivatives as organic semiconductors, field-effect transistors (FETs) of these derivatives were fabricated using a soluble process. As shown in **Figure 5**, FET devices composed of CE4T and CB4T showed typical p-channel responses, and the output curves showed excellent saturation behavior. The field-effect mobilities of the devices based on CE4T and CB4T were 1.14×10^{-2} cm^2 V^{-1} s^{-1} ($I_{on}/I_{off} = 4.76 \times 10^5$) and 1.55×10^{-2} cm^2 V^{-1} s^{-1} ($I_{on}/_{off} = 2.06 \times 10^6$) in the saturation regime, whereas the field-effect mobilities of devices based on DCE4T and DCB4T were 3.10×10^{-4} cm^2 V^{-1} s^{-1}) ($I_{on}/I_{off} = 2.05 \times 10^2$) and 2.35×10^{-5} cm^2 V^{-1} s^{-1} ($I_{on}/_{off} = 8.04 \times 10$).

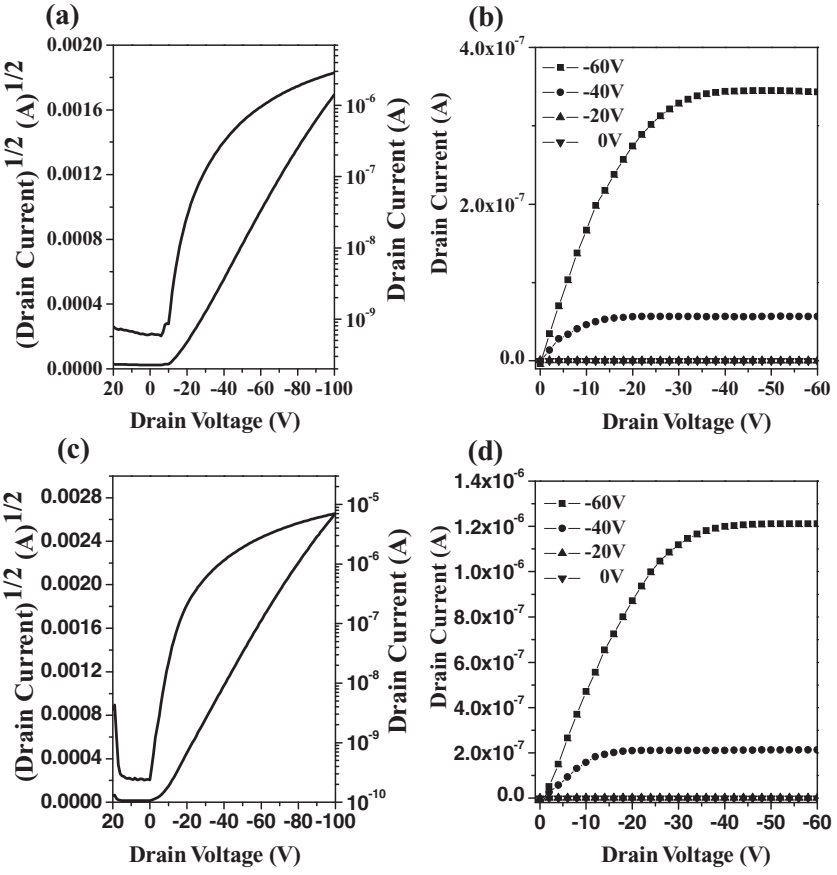

Figure 5. Transfer and output characteristics of OFETs based on CE4T (a and b) and CB4T (c and d).

A structural analysis, based on the UV–vis absorption and GIWAXS results, revealed specific features that explained the pronounced differences in field-effect mobilities between the cyclohexylated and dicyclohexylated quaterthiophene derivatives. Clear correlations were observed, as expected: H-aggregation (CB4T and CE4T) produced higher charge carrier mobilities, and J-aggregation (DCB4T and DCE4T) produced lower mobilities. As the number of molecules stacked in parallel increased to produce a large area of π-overlap, hole mobility among adjacent molecules improved, thereby producing higher field-effect mobilities in the devices. In addition, the packing patterns on substrates, shown in Figure 4, revealed that the orientations of cyclohexylated or dicyclohexylated quaterthiophene molecules in the lattices were different. In other words, lattices composed of dicyclohexylated quaterthiophenes were tilted, and, thus, the thin films were expected to contain some defects because the orientations in the tilted lattices were not uniform. Dicyclohexylated quaterthiophenes were found to stack by a head-to-tail arrangement. Therefore, the connectivity in the dicyclohexylated quaterthiophene film was poorer than the connectivity in the cyclohexylated quaterthiophenes, resulting in different field-effect mobilities in films composed of each type of substituent molecules.

The tendency that the charge carrier mobility of FET devices composed of cyclohexylated quaterthiophenes is higher than that of devices based on dicyclohexylated quaterthiophenes is opposite to that previously reported.[25] The difference of tendency of charge carrier mobility may come from substituent alkyl groups. It is well known that lipophilic alkyl chain at the α-position of oligothiophenes can induce stronger intermolecular interaction between adjacent molecules by Van der Waals interactions.[26] On the other hand, in our study, the bulky side groups generate steric hindrance and the bulky side groups push each molecule away. Therefore, cyclohexylated quaterthiophenes are vertically aligned in a face-to-face packing structure, and dicyclohexylated quaterthiophenes are diagonally packed on the substrate.

H-aggregation has another advantage over thin film transistors (TFTs) in that the reproducibility of device properties with this type of molecular stacking is superior. The high crystallinity of cyclohexylated quaterthiophenes with H-type packing produced remarkably uniform and reproducible TFT performances. We compared the reproducibility of charge carrier mobility in cyclohexylated and dicyclohexylated quaterthiophenes, poly[9,9-dioctylfluorenyl-2,7-diyl]-*co*-(bithiophene) (F8T2) and 6,13-bis(triisopropyl-silylethynyl) pentacene (TIPS-pentacene)-based TFTs. We measured the performances of dozens of transistors. TFTs based on dicyclohexylated quaterthiophenes yielded poor TFT performance, such that it was difficult to compare the performance distribution with the distributions of other materials. Although it is well-known that drop-cast slow solvent-drying methods for TIPS-pentacene films produce high mobilities that exceed 1 $cm^2\ V^{-1}\ s^{-1}$,[27] the poor performance reproducibility in such films forced us to use spin-coating methods that yielded relatively lower mobilities, simply to compare the reproducibility of TFT performance.

As shown in **Figure 6**a and b, the distribution of mobilities in TIPS-pentacene TFTs fabricated by spin-coating was very broad. The distributions of mobilities in CE4T and CB4T TFTs were remarkably narrower than those of TIPS-pentacene and F8T2 TFTs. Devices based on cyclohexylated quaterthiophenes yielded the most reproducible data. The standard deviations of CE4T, CB4T, and F8T2 TFT mobilities were 7.67×10^{-4}, 1.02×10^{-3} and 2.54×10^{-3}. Furthermore, we fabricated a 4 inch diameter sample via one-step spin-coating of CE4T to highlight the superior performance reproducibility of films based on this molecule. The results are shown in **Figure 7**. Over almost the whole area, a constant FET performance (equal to the average value) was obtained. Therefore, devices based on cyclohexylated quaterthiophenes yielded good performance reproducibility by improving the molecular ordering within the thin films as a result of H-aggregation.

3. Conclusions

We designed four types of quaterthiophene derivatives with end-groups composed of DCE4T, DCB4T, CE4T, and CB4T.

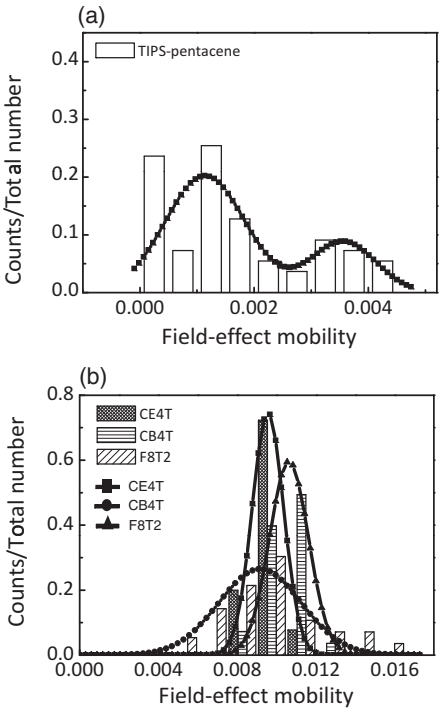

Figure 6. The distribution of field-effect mobilities of OFETs based on a) TIPS-pentacene, b) CE4T, CB4T, and F8T2.

These four materials were suitable for soluble processing, suggesting that all materials had good solubility and good wettability in nonpolar solvents. Interestingly, we found that quaterthiophene derivatives with asymmetrically substituted cyclohexyl end-groups, CE4T and CB4T, produced H-type aggregation that differed from the aggregation observed for materials with symmetrically substituted cyclohexyl end-groups, DCE4T and DCB4T, or other conventional molecular semiconductors. This observation was made on the basis of an analysis of the absorption and diffraction measurements. The large π-overlap area in H-type aggregation materials produced FET mobilities in the asymmetrical molecules that were clearly higher than those measured in symmetrical molecules. In addition, good ordered packing caused by H-aggregation produced TFTs with stable morphologies and highly reproducible performances. These findings revealed that, through strategic molecular structural design, H-aggregation can be introduced to molecular semiconductors to achieve higher performance and better reproducibility in organic electronics.

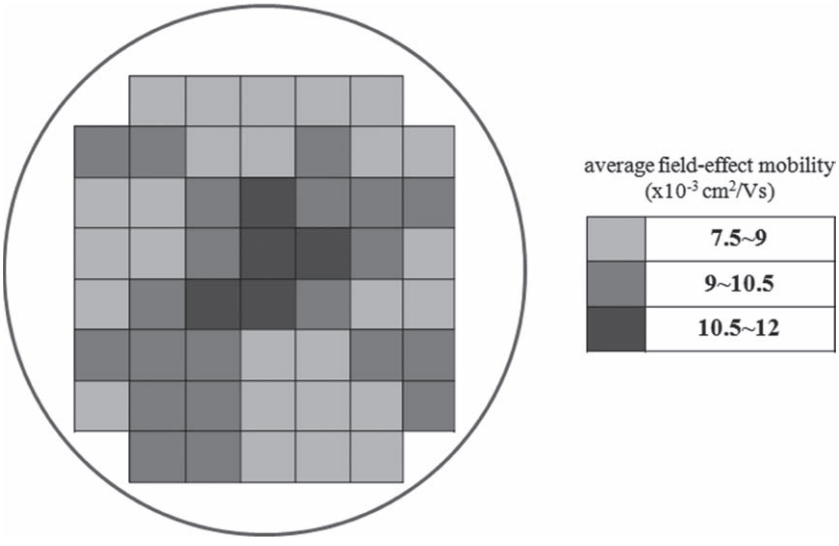

Figure 7. Four inch diameter sample using CE4T. Each sample size was 1 cm × 1 cm, and the number of samples was 52. The gradation of colors shows the average field-effect mobility in each sample, and 4 transistors were measured in each sample.

4. Experimental Section

Materials: All reagents were purchased from Aldrich or Alfa, and chemical agents were purchased from Aldrich, Acros, and Lancaster. Tetrahydrofuran (THF) and diethyl ether were distilled over sodium in the presence of benzophenone to remove water.[28] Toluene was distilled over calcium hydride prior to use to ensure that it was anhydrous. Chloroform, dichloromethane, and methanol were used without further purification. The reagents 5,5'-dibromo-[2,2']bithiophene, 5-bromo-[2,2';5',2'']terthiophene, and (4-bromo-butyl)-cyclohexane were synthesized according to known procedures.[28–31]

Measurements: The ^{1}H-NMR spectra were recorded using a Bruker AM-200 spectrometer. FT-IR spectra were measured using a Bomen Michelson series FT-IR spectrometer. The melting points were determined using an Electrothermal Mode 1307 digital analyzer. Thermogravimetric analysis (TGA) was performed under nitrogen using a TA Instruments 2050 thermogravimetric analyzer. The sample was heated at a 10 °C min^{-1} heating rate from 30 °C to 700 °C. Differential scanning calorimetry (DSC) was conducted under nitrogen using a TA Instruments 2100 differential scanning calorimeter. The samples were heated at 10 °C min^{-1} from 30 °C to 300 °C. UV-vis absorption spectra were measured using a Perkin-Elmer LAMBDA-900 UV/vis/IR spectrophotometer.

Synthesis of (2-Chloro-ethyl)-cyclohexane: 2-Cyclohexyl-ethanol (20.0 g, 0.16 mol) was added slowly to a mixture of purified thionyl chloride (46.4 g, 0.39 mol) and pyridine (24.7 g, 0.31 mol) with cooling at 0 °C over an ice bath. After one hour, the solution was heated to 115 °C and stirred overnight. After the mixture was cooled to room temperature, it was quenched with ice water and extracted with CH_2Cl_2. The combined organic layer was dried over anhydrous magnesium sulfate. The solvent was removed by rotary evaporation, and the resulting residue was purified by vacuum fractional distillation to give the pure product as a colorless liquid. Yield: 12.4 g (54.4%). BP: 50–52 °C/3 mmHg. ^{1}H NMR (300 MHz, CDCl3), δ_H 3.5 (t, 2H), 1.7 (m,7H), 1.65 (m, 1H), 1.2 (m, 3H), 0.9 (m, 2H).

Synthesis of 2-(2-Cyclohexyl-ethyl)-thiophene: Magnesium (2.18 g, 89.6 mmol) was added to a three-neck flask, and water and air were removed. Subsequently, (2-chloro-ethyl)-cyclohexane (12.0 g, 81.5 mmol) and diethyl ether (250 mL) were added dropwise to the flask. The reactant mixture was refluxed for 1 h. The resulting Grignard reagent solution was then added dropwise to a solution of 2-bromothiophene (13.29 g, 81.5 mmol) and Ni(dppp)Cl_2 (where dppp is diphenylphosphinopropane) (0.44 g, 0.8 mmol) with cooling over an ice bath. The mixture was then stirred overnight at room temperature and quenched with 1 N HCl. The organic layer was separated and extracted with ether. The combined ether

solution was washed with H_2O three times and dried over anhydrous $MgSO_4$. After removal of the solvent, the resulting liquid was subjected to purification by flash chromatography using silica gel with hexane as the eluent. Yield: 6.65 g (42.1%). ^{1}H NMR (300 MHz, $CDCl_3$), δ_H 7.14 (m, 1H), 6.96 (m, 1H), 6.81 (m, 1H), 2.88 (t, 2H), 1.58–1.82 (m, 7H), 1.25 (m, 4H), 0.97 (t, 2H).

Synthesis of Tributyl-[5-(2-cyclohexyl-ethyl)-thiophen-2-yl]-stannane: BuLi (2.5 M in hexane) (14.45 mL, 35.9 mmol) was added slowly to a solution of 2-(2-cyclohexyl-ethyl)-thiophene (6.65 g, 34.2 mmol) in THF (70 mL) at –78 °C. After lithiation, tributyltin chloride (11.76 g, 36.1 mmol) was added to the mixture at –78 °C. The reaction was allowed to warm to room temperature and stirred overnight. After normal workup, the organic layer was separated and extracted with hexane. The combined hexane solution was washed with saturated $NaHCO_3$ three times and dried over anhydrous $MgSO_4$. After removal of the solvent, the resulting crude product was used without further purification. Yield: 11.58 g (80%). ^{1}H NMR (300 MHz, $CDCl_3$), δ_H 7.01 (d, 1H), 6.91 (d, 1H), 2.89 (t, 2H), 1.56–1.69 (m, 7H), 1.32–1.39 (m, 18H), 1.21 (m, 4H), 1.07–1.12 (m, 9H), 0.93 (t, 2H).

Synthesis of 5,5'''-Dicyclohexyl-ethyl-[2,2';5',2'';5'',2''''-quaterthiophene (DCE4T): Tributyl-[5-(2-cyclohexyl-ethyl)-thiophen-2-yl]-stannane (2.74 g, 5.67 mmol) and 5,5'-dibromo-[2,2']-bithiophene (0.80 g, 2.46 mmol) were added to toluene (30 mL) in a one-neck flask equipped with a condenser. After three freeze-pump-thaw cycles, $Pd(PPh_3)_4$ (0.17 g, 6 mol%) was added to the mixture under a nitrogen atmosphere, and the solution was heated to 100 °C for 24 h. The mixture was cooled to room temperature, filtered, and washed with hexane and THF to the remove starting material and any monocoupled product. The resulting solid was subjected to purification by chromatography using silica gel with toluene as the eluent to afford nearly pure solid product. This solid was further purified by recrystallization from MeOH–$CHCl_3$ to give yellow-orange crystals. Yield: 0.83 g (61.2%). ^{1}H NMR (300 MHz, CDCl3), δ_H 7.05 (d, 1H), 7.00 (t, 2H), 6.69 (t, 1H), 2.83 (t, 2H), 1.56–1.80 (m, 7H), 1.23 (m, 4H), 0.95 (m, 2H). MS (EI) m/z: 550 (M+).

Synthesis of 5-(2-Cyclohexyl-ethyl)-[2,2';5',2'';5'',2''''-quaterthiophene (CE4T): Tributyl-[5-(2-cyclohexyl-ethyl)-thiophen-2-yl]-stannane (3.0 g, 6.20 mmol) and 5-bromo-[2,2';5',2'']terthiophene (2.03 g, 6.20 mmol) were added to toluene (40 mL) in a one-neck flask equipped with a condenser. After three freeze-pump-thaw cycles, $Pd(PPh_3)_4$ (0.43 g, 6 mol%) was added to the mixture under a nitrogen atmosphere, and the solution was heated to 90 °C for 24 h. The mixture was cooled to room temperature, quenched with water, and extracted with $CHCl_3$. The combined organic layer was dried over anhydrous magnesium sulfate. After removing the solvent, the resulting solid was subjected to purification by chromatography using silica gel with hexane as the eluent. Finally, the solid was recrystallized from MeOH–CH_2Cl_2 to give the pure target compound as yellow crystals. Yield: 1.88 g (69.0%). ^{1}H NMR (300 Hz, CDCl3), δ_H 7.23 (d, 1H), 7.19 (d, 1H), 7.05 (m, 6H), 6.70 (d, 1H), 2.81 (t, 2H), 1.62–1.79 (m, 7H), 1.25 (m, 4H), 0.89 (m, 2H). MS (EI) m/z: 440 (M+)

Synthesis of 2-(4-cyclohexyl-butyl)-thiophene: Magnesium (2.16 g, 89.0 mmol) was added to a 3-neck flask, and water and air were removed. Subsequently, (4-bromo-butyl)-cyclohexane (15 g, 68.4 mmol) and diethyl ether (200 mL) were added dropwise to the flask. The reactant mixture was refluxed for 2 h. The resulting Grignard reagent solution was then added dropwise to the solution of 2-bromothiophene (11.16 g, 68.4 mmol) and Ni(dppp)Cl_2 (where dppp is diphenylphosphinopropane) (2.22 g, 6 mol%) with cooling over an ice bath. The mixture was then stirred overnight at room temperature and quenched with 1 N HCl. The organic layer was separated and extracted with ether. The combined ether solution was washed with H_2O three times and dried over anhydrous $MgSO_4$. After removing the solvent, the resulting liquid was subjected to purification by flash chromatography using silica gel with hexane as the eluent. Yield: 6.19 g (40.7%). ^{1}H NMR (300 MHz, $CDCl_3$), δ_H 7.16 (m, 1H), 6.95 (m, 1H), 6.83 (m, 1H), 2.85 (t, 2H), 1.72 (m, 7H), 1.39 (m, 2H), 1.25 (m, 6H), 0.91 (d, 2H).

Synthesis of Tributyl-[5-(4-cyclohexyl-butyl)-thiophen-2-yl]-stannane: BuLi (2.5 M in hexane) (6 mL, 14.91 mmol) was added slowly to a solution of 2-(4-cyclohexyl-butyl)-thiophene (2.77 g, 14.2 mmol) in THF (30 mL) at –78 °C. After lithiation, tributyltin chloride (4.88 g, 14.98 mmol) was added to the mixture at –78 °C. The reaction was allowed to warm to room temperature and stirred overnight. After normal workup, the organic layer was separated and extracted with hexane. The combined hexane solution was washed with saturated $NaHCO_3$ three times and dried over anhydrous $MgSO_4$. After removal of the solvent, the crude product was used without further purification. Yield: 5.83 g (80%). ^{1}H NMR (300 MHz, $CDCl_3$), δ_H 7.01 (d, 1H), 6.93 (d, 1H), 2.85 (t, 2H), 1.69 (m, 7H), 1.37 (m, 20H), 1.23 (m, 6H), 1.09 (m, 9H), 0.89 (d, 2H).

Synthesis of 5,5'''-Dicyclohexyl-butyl-[2,2';5',2'';5'',2''']quaterthiophene (DCB4T): Tributyl-[5-(4-cyclohexyl-butyl)-thiophen-2-yl]-stannane (2.96 g, 5.8 mmol) and 5,5'-dibromo-[2,2']bithiophene (0.75 g, 2.3 mmol) were added to toluene (20 mL) in a one-neck flask equipped with a condenser. After three freeze-pump-thaw cycles, $Pd(PPh_3)_4$ (0.16 g, 6 mol%) was added to the mixture under a nitrogen atmosphere, and the solution was heated to 100 °C for 24 h. Subsequently, the mixture was cooled to room temperature, quenched with water, and extracted with $CHCl_3$. The combined organic layer was dried over anhydrous magnesium sulfate. After removing the solvent, the resulting solid was subjected to purification by chromatography using silica gel with hexane as the eluent to afford a nearly pure solid product. This solid was further purified by recrystallization from MeOH–$CHCl_3$ to give yellow crystals. Yield: 0.84 g (59.8%). ^{1}H NMR (300 MHz, $CDCl_3$), δ_H 7.05 (d, 1H), 7.00 (t, 2H), 6.69 (d, 1H), 2.81 (t, 2H), 1.68 (m, 7H), 1.38 (m, 2H), 1.22 (m, 6H), 0.89 (d, 2H). MS (EI) m/z: 607 (M+)

Synthesis of 5-(2-Cyclohexyl-butyl)-[2,2';5',2'';5'',2'''']-quaterthiophene (CB4T): Tributyl-[5-(2-cyclohexyl-ethyl)-thiophen-2-yl]-stannane (2.36 g, 4.6 mmol) and 5-bromo-[2,2';5',2'']terthiophene (1.51 g, 4.6 mmol) were added to toluene (30 mL) in a one-neck flask equipped with a condenser. After three freeze–pump–thaw cycles, $Pd(PPh_3)_4$ (0.32 g, 6 mol%) was added to the mixture under a nitrogen atmosphere, and the solution was heated to 90 °C for 24 h. After the mixture was cooled to room temperature, it was quenched with water and extracted with $CHCl_3$. The combined organic layer was dried over anhydrous magnesium sulfate. After removing the solvent, the resulting solid was subjected to purification by chromatography using silica gel with hexane as the eluent. Finally, this solid was recrystallized from MeOH–CH_2Cl_2 to give the pure target compound as yellow crystals. Yield: 1.54 g (71.2%). ^{1}H NMR (300 MHz, $CDCl_3$), δ_H 7.23 (t, 1H), 7.18 (d, 1H), 7.06 (m, 6H), 6.69 (d, 1H), 2.81 (t, 2H), 1.68 (m, 7H), 1.38 (m, 2H), 1.22 (m, 6H), 0.89 (d, 2H). MS (EI) m/z: 468 (M+).

Fabrication and Characterization of the OFET Devices: Top-contact OFETs were fabricated on a common gate of highly n-doped silicon with a 300 nm thick thermally grown SiO_2 dielectric layer. The octadecyltrichlorosilane monolayer was treated in toluene solution for 2 h. Solutions of the organic semiconductors were spin-coated at 2000 rpm from 0.7 wt.% chloroform solutions to form thin films with a nominal thickness of 45 nm, confirmed using a surface profiler (Alpha Step 500, Tencor). Gold source and drain electrodes were evaporated on top of the semiconductor layers (100 nm).[32] For all measurements, we used channel lengths (L) of 100 μm and channel widths (W) of 2000 μm. The electrical characteristics of the FETs were measured in air using both Keithley 2400 and 236 source/measure units. Field-effect mobilities were extracted in the saturation regime from the slope of the source–drain current. X-ray diffraction (XRD) studies were performed using the 4C1 and 4C2 beamlines at the Pohang Accelerator Laboratory (PAL). The measurements were carried out with a sample-to-detector distance of 136 mm. Data were typically collected for ten seconds using an X-ray radiation source of $\lambda = 0.138$ nm with a 2D charge-coupled detector (CCD) (Roper Scientific, Trenton, NJ, USA). The samples were mounted onto a home-built z-axis goniometer equipped with a vacuum chamber. The incidence angle a_i of the X-ray beam was set to 0.14°, which is intermediate between the critical angles of the films and the substrate ($a_{c,f}$ and $a_{c,s}$).

Supporting Information

Supporting Information is available from the Wiley Online Library or from the author.

Acknowledgements

S.-O.K. and T.K.A. contributed equally to this work. This work was supported by a grant (F0004011–2010-33) from the Information Display R&D Center, one of the 21st Century Frontier R&D Program funded by the Ministry of Knowledge Economy and Basic Science Research Program; by a grant (2010–000826) from the National Research Foundation (NRF) funded by the Ministry of Education, Science and Technology and the Ministry of Knowledge Economy (MKE) and Korea Institute for Advancement in Technology (KIAT) through the Workforce Development Program in Strategic Technology.

Received: November 10, 2010
Revised: January 16, 2011
Published online: March 17, 2011

[1] J. Locklin, D. Li, W. S. C. B. Mannsfeld, E. J. Borkent, H. Meng, R. Advincula, Z. Bao, *Chem. Mater.* **2005**, *17*, 3366.

[2] a) H. Meng, J. Zheng, A. J. Lovinger, B. C. Wang, P. G. Van Patten, Z. Bao, *Chem. Mater.* **2003**, *15*, 1778; b) M. Mushrush, A. Facchetti, M. Lefenfeld, H. E. Katz, T. J. Marks, *J. Am. Chem. Soc.* **2003**, *125*, 9414; c) A. Facchetti, M. Mushrush, H. E. Katz, T. J. Marks, *Adv. Mater.* **2003**, *15*, 33; d) D. M. DeLongchamp, S. Sambasivan, D. A. Fischer, E. K. Lin, P. Chang, A. R. Murphy, J. Frchet, V. Subramanian, *Adv. Mater.* **2005**, *17*, 2340.

[3] a) M. Pasini, S. Destri, W. Porzio, C. Botta, U. Giovanella, *J. Mater. Chem.* **2003**, *13*, 807; b) M. Suzuki, M. Fukuyama, Y. Hori, S. Hotta, *J. Appl. Phys.* **2002**, *91*, 5706.

[4] K. Hara, M. Kurashige, Y. Dan-Oh, C. Kasada, A. Shinpo, S. Suga, K. Sayama, H. Arakawa, *New J. Chem.* **2003**, *27*, 783.

[5] a) H. S. Kim, Y. H. Kim, T. H. Kim, Y. Y. Noh, S. M. Pyo, M. H. Yi, D. Y. Kim, S.-K. Kwon, *Chem. Mater.* **2007**, *19*, 3561; b) Q. Zhao, T. H. Kim, J. W. Park, S. O. Kim, S. O. Jung, J. W. Kim, T. Ahn, Y. H. Kim, M. H. Yi, S. K. Kwon, *Adv. Mater.* **2008**, *20*, 4868; c) J. W. Park, D. H. Lee, D. S. Chung, D. M. Kang, Y. H. Kim, C. E. Park, S.-K. Kwon, *Macromolecules* **2010**, *43*, 2118; d) D. S. Chung, S. J. Lee, J. W. Park, D. B. Choi, D. H. Lee, J. W. Park, S. C. Shin, Y. H. Kim, S.-K. Kwon, C. E. Park, *Chem. Mater.* **2008**, *20*, 3450; e) Y. N. Li, T. H. Kim, Q. H. Zhao, E. K. Kim, S. H. Han, Y. H. Kim, J. Jang, S. -K. Kwon, *J. Polym. Sci., Part A: Polym. Chem.* **2008**, *46*, 5115; f) D. S. Chung, J. W. Park, S. O. Kim, K. Heo, C. E. Park, Y. H. Kim, S.-K. Kwon, *Chem. Mater.* **2009**, *21*, 5499; g) M. J. Lee, M. S. Kang, M. K. Shin, J. W. Park, D. S. Chung, C. E. Park; S.-K. Kwon; Y. H. Kim, *J. Polym. Sci., Part A: Polym. Chem.* **2010**, *48*, 3942; h) J. U. Ju, D. S. Chung, S. O. Kim, S. O. Jung, C. E. Park, Y. H. Kim, S.-K. Kwon, *J. Polym. Sci., Part A: Polym. Chem.* **2009**, *47*, 1609; i) T. T. M. Dang, S. J. Park, J. W. Park, D. S. Chung, C. E. Park, Y. H. Kim, S. -K. Kwon, *J. Polym. Sci., Part A: Polym. Chem.* **2007**, *45*, 5277.

[6] R. P. Ortiz, A. Facchetti, T. J. Marks, J. Casado, M. Z. Zgierski, M. Kozaki, V. Hernandez, J. T. L. Navarrete, *Adv. Funct. Mater.* **2009**, *19*, 386.

[7] H. Yan, Z. Chen, Y. Zheng, C. Newman, J. R. Quinn, F. Dotz, M. Kastler, A. Facchetti, *Nature* **2009**, *457*, 679.

[8] W. Zhang, J. Smith, S. E. Watkins, R. Gysel, M. McGehee, A. Salleo, J. Kirkpatrick, S. Ashraf, T. Anthopoulos, M. Heeney, I. McCulloch, *J. Am. Chem. Soc.* **2010**, *132*, 11437.

[9] A. A. Virkar, S. Mannsfeld, Z. Bao, N. Stingelin, *Adv. Mater.* **2010**, *22*, 3857.

[10] C. Nogues, P. Lang, B. Desbat, T. Buffeteau, L. Leiserowitz, *Langmuir* **2008**, *24*, 8458.

[11] a) P. Frere, J. M. Raimundo, P. Blanchard, J. Delaunay, P. Richomme, J. L. Sauvajol, J. Garin, J. Orduna, J. Roncali, *J. Org. Chem.* **2003**, *68*, 5357; b) J. Z. Wang, Z. H. Zheng, H. W. Li, W. T. S. Huck, H. Sirringhaus, *Nat. Mater.* **2004**, *3*, 171; c) A. Afzali, T. L. Breen, C. R. Kagan, *Chem. Mater.* **2002**, *14*, 1742.

[12] D. J. Fichou, *Mater. Chem.* **2000**, *10*, 571.

[13] S. E. Fritz, S. Mohapatra, B. T. Holmes, A. M. Anderson, C. F. Prendergast, C. D. Frisbie, M. D. Ward, M. F. Toney, *Chem. Mater.* **2007**, *19*, 1355.

[14] a) J. H. Choi, D. W. Cho, H. J. Park, S.-H. Jin, S. Jung, M. Yi, C. K. Song, U. C. Yoon, *Synth. Met.* **2009**, *159*, 15; b) M.–H. Yoon, A. Facchetti, C. E. Stern, T. J. Marks, *J. Am. Chem. Soc.* **2006**, *128*, 5792; c) S. Paek, J. Lee, J. M. Ko, H. S. Lim, J. Lim, S. H. Cho, J. Y. Lee, C. Lee, *Mol. Cryst. Liq. Cryst.* **2009**, *504*, 52–58.

[15] F. C. Spano, *Acc. Chem. Res.* **2010**, *43*, 429.

[16] a) C. Reesea, Z. Bao, *Mater. Today* **2007**, *10*, 20; b) A. R. Murphy, J. M. J. Frechet, *Chem. Rev.* **2007**, *107*, 1066; c) A. L. Briseno, J. Aizenberg, Y.-J. Han, R. A. Penkala, H. Moon, A. J. Lovinger, C. Kloc, Z. Bao, *J. Am. Chem. Soc.* **2005**, *127*, 12164; c) D. S. Chung, J. W. Park, J.-H. Park, D. Moon, G. H. Kim, H.-S. Lee, D. H. Lee, H.-K. Shim, S.-K. Kwon, C. E. Park, *J. Mater. Chem.* **2010**, *20*, 524.

[17] S. J. Park, S. O. Kim, S. O. Jung, M. H. Yi, Y. H. Kim, S. -K. Kwon, *J. Electron. Mater.* **2009**, *186*, 1543

[18] H. Menzel, B. Weichart, *Langmuir* **1994**, *10*, 1926.

[19] a) F. C. Spano, *Annu. Rev. Phys. Chem.* **2006**. *57*, 217; b) F. Meinardi, M. Cerminara, A. Sassella, R. Bonifacio, R. Tubino, *Phys. Rev. Lett.* **2003**, *91*, 247401.

[20] P. Atkins, J. Paula, *Atkins' Physical Chemistry*, 7th ed., Oxford University Press, New York, **2002**.

[21] a) J. Frank, E. Teller, *J. Chem. Phys.* **1938**, *6*, 861; b) J. Kang, O. Kaczmarek, J. Liebscher, L. Dahne, *Int. J. of Polym. Sci.* **2010**, 2010.

[22] a) B. Lee, I. Park, J. Yoon, S. Park, J. Kim, K.–W. Kim, T. Chang, M. Ree, *Macromolecules* **2005**, *38*, 4311; b) P. Muller-Buschbaum, *Anal. Bioanal. Chem.* **2003**, *376*, 3

[23] R.–J. Roe, *Methods of X-ray and Neutron Scattering in Polymer Science*, 1st ed., Oxford University Press, New York **2000**.

[24] T. J. Shin, H. Yang, M. –M. Ling, J. Locklin, L. Yang, B. Lee, M. E. Roberts, A. B. Mallik, Z. Bao, *Chem. Mater.* **2007**, *19*, 5882.

[25] A.-L. Deman, J. Tardy, Y. Nicolas, P. Blanchard, J. Roncali, *Synth. Met.* **2004**, *146*, 365

[26] a) H.E. Katz, A. Dodabalapur, L. Torsi, D. Elder, *Chem. Mater.* **1995**, *7*, 2238; b) C. D. Dimitrakopoulos, B. K. Furman, T. Graham, S. Hedge, S. Purushothaman, *Synth. Met.* **1998**, *92*, 47; c) R. Bourguiga, F. Garnier, G. Horowitz, R. Hajlaoui, P. Delannoy, M. Hajlaoui, H. Bouchriha, *Eur. Phys. J. AP.* **2001**, *14*, 121.

[27] a) S. K. Park, T. N. Jackson, J. E. Anthony, D. A. Mourey, *Appl. Phys. Lett.* **2007**, *91*, 3514; b) C. S. Kim, S. Lee, E. D. Gomez, J. E. Anthony, Y. -L. Loo, *Appl. Phys. Lett.* **2008**, *93*, 3302.

[28] H. Andringa, J. Hanekamp, L. Brandsma, *Synth. Commun.* **1990**, *20*, 2349.

[29] Y. A. Getmanenko, R. J. Twieg, *Org. Chem.* **2008**, *73*, 831.

[30] D. Didier, S. Sergeyev, Y. H. Geerts, *Tetrahedron* **2007**, *63*, 941–946.

[31] R. Hajlaoui, D. Fichou, G. Horowitz, B. Nessakh, M. Constant, F. Garnier, *Adv. Mater.* **1997**, *7*, 557

[32] S. J. Park, S. O. Kim, S. O. Jung, M. H. Yi, Y. H. Kim, S.-K. Kwon, *J. Electron. Mater.* **2009**, *186*, 1543.